Title
Shelterin Protects Chromosome Ends by Compacting Telomeric Chromatin

Journal
Cell, 164(4)

ISSN
0092-8674

Authors
Bandaria, Jigar N
Qin, Peiwu
Berk, Veysel
et al.

Publication Date
2016-02-01

DOI
10.1016/j.cell.2016.01.036

Peer reviewed

HHS Public Access

Author manuscript

Cell. Author manuscript; available in PMC 2017 February 11.

Published in final edited form as:

Cell. 2016 February 11; 164(4): 735–746. doi:10.1016/j.cell.2016.01.036.

Shelterin Protects Chromosome Ends by Compacting Telomeric Chromatin

Jigar N. Bandaria[1,2], **Peiwu Qin**[1], **Veysel Berk**[2,3], **Steven Chu**[3], and **Ahmet Yildiz**[1,2,*]

[1]Department of Physics, University of California, Berkeley, CA 94720, USA

[2]Department of Molecular and Cell Biology, University of California, Berkeley, CA 94720, USA

[3]Department of Physics, Stanford University, Stanford, CA 94305, USA

SUMMARY

Telomeres, repetitive DNA sequences at chromosome ends, are shielded against the DNA damage response (DDR) by the shelterin complex. To understand how shelterin protects telomere ends, we investigated the structural organization of telomeric chromatin in human cells using super-resolution microscopy. We found that telomeres form compact globular structures through a complex network of interactions between shelterin subunits and telomeric DNA, and not by DNA methylation, histone deacetylation or histone trimethylation at telomeres and subtelomeric regions. Mutations that abrogate shelterin assembly or removal of individual subunits from telomeres cause up to a 10-fold increase in telomere volume. Decompacted telomeres become more accessible to telomere-associated proteins and accumulate DDR signals. Recompaction of telomeric chromatin using an orthogonal method displaces DDR signals from telomeres. These results reveal the chromatin remodeling activity of shelterin and demonstrate that shelterin-mediated compaction of telomeric chromatin provides robust protection of chromosome ends against the DDR machinery.

INTRODUCTION

The natural ends of eukaryotic chromosomes are prone to being misrecognized as DNA breaks, which poses a unique challenge for genome integrity and cell viability. Cells overcome this challenge by forming a protective structure at chromosome ends comprising a tandem array of telomeric DNA repeats and telomere binding proteins (Palm and de Lange, 2008). Defects in the protection of telomeres have been implicated in cancer and aging (Blasco, 2013).

*Correspondence to: yildiz@berkeley.edu.

SUPPLEMENTAL INFORMATION

Supplemental Information includes Supplemental Experimental Procedures, one table, seven figures, and four movies.

AUTHOR CONTRIBUTIONS:

A.Y. and J.B. designed the experiments, J.B., V.B. and S.C. designed and built the optical setup, J.B. and P.Q. conducted the experiments and data analysis, A. Y. and J.B. wrote the manuscript.

In humans, telomeres consist of 2–20 kb of double-stranded TTAGGG repeats (dsTEL) with terminal 50–500 nucleotide long 3′ single-stranded G-overhangs (ssTEL) (Palm and de Lange, 2008). Human telomeres associate with the shelterin complex, which contains six proteins (Figure 1A). TRF1 and TRF2 are homodimeric proteins that bind to dsTEL with their C-terminal MYB domains (Fairall et al., 2001; Griffith et al., 1999). RAP1 is recruited through its interaction with TRF2 (Palm and de Lange, 2008). POT1 binds specifically to ssTEL and forms a heterodimer with TPP1 (O'Connor et al., 2006). TIN2 is a hub that interacts with TRF1, TRF2 and POT1/TPP1 (O'Connor et al., 2006; Ye et al., 2004), mediating the assembly of the entire complex. Perturbation or removal of individual shelterin subunits have been shown to activate specific DDR pathways. TRF1 prevents the activation of both ataxia telangiectasia mutated (ATM) and ataxia telangiectasia and Rad3 related (ATR) pathways (Martinez et al., 2009). TRF2, RAP1, and POT1/TPP1 inhibit the activation of ATM (Karlseder et al., 2004), homology-directed recombination (HDR) (Sfeir et al., 2010) and ATR (Liu et al., 2004) pathways, respectively.

The mechanism of telomere end protection has been attributed primarily to TRF2-mediated sequestration of the 3′ overhang within large duplex loops (t-loops) (Doksani et al., 2013; Griffith et al., 1999). Several observations have suggested that other mechanisms must also exist for the robust protection observed at telomeres. First, the removal of shelterin subunits other than TRF2 from telomeres also leads to the activation of specific DDR pathways (Sfeir and de Lange, 2012; Takai et al., 2011), although t-loops still form in their absence (Doksani et al., 2013). Second, short telomeres are more prone to DDR induction than longer telomeres (Herbig et al., 2004; Smogorzewska et al., 2000), although they are long enough to form t-loops (Doksani et al., 2013; Munoz-Jordan et al., 2001). Thus, the mechanism by which shelterin subunits and the length of dsTEL tracts contribute to telomere end capping remains unclear.

Several *in vitro* studies have suggested a DNA remodeling role for shelterin. TRF1 and TRF2, which are highly abundant at telomeres (Palm and de Lange, 2008), pair and loop distal telomeric tracts (Griffith et al., 1999) and condense short telomeric fragments *in vitro* (Poulet et al., 2012), but it is not known whether these proteins play a major role in high-order remodeling of telomeric chromatin *in vivo*. More critically, a causal relationship between chromatin remodeling activities of shelterin and telomere protection from damage has not yet been established.

Telomeres also possess features of heterochromatin, such as the enrichment of trimethylated histones H3K9 and H4K20, and the presence of the heterochromatin protein HP1 (Benetti et al., 2007). Heterochromatin formation protects chromosome integrity and limits the access of DNA-binding proteins in nontelomeric regions (Lorat et al., 2012; Murga et al., 2007). Similarly, hypercondensation of telomeric chromatin may limit the access of DDR signals to telomere ends (Benetti et al., 2007). However, telomeric nucleosomes are highly mobile (Cacchione et al., 1997; Ichikawa et al., 2014; Pisano et al., 2007) and their occupancy is negatively regulated by TRF1 and TRF2 (Galati et al., 2012; Pisano et al., 2010). Therefore, it remains unclear whether posttranslational modifications of DNA and histones at telomeres and subtelomeric regions are primarily responsible for hypercondensation of telomeric chromatin. Telomeres are unsuitable for study by chromosome conformation capture

methods due to their homogeneous sequence (Nagano et al., 2013). Therefore, alternative approaches are needed to gain insight into the structure of telomeric chromatin.

Here, we investigated how shelterin affects the structural organization of telomeric chromatin in human cells using super-resolution microscopy and whether its remodeling activity directly protects telomere ends against DDR accumulation. We observed that telomeres form compact chromatin structures *in vivo* through specific protein-protein and protein-DNA interactions between shelterin subunits and telomeric DNA. The compaction of telomeric chromatin is essential for robust protection of chromosome ends by limiting the accessibility of the DDR machinery. Our results demonstrate that shelterin plays a critical role in the condensation of telomeric chromatin inside cells and that DNA compaction directly leads to the reduction in DDR signaling at telomeres.

RESULTS

Super-resolution imaging of human telomeres

To directly visualize human telomeres, we fused a photoactivable monomeric GFP, mEos2 (McKinney et al., 2009) to the N-terminus of TRF1 and TRF2 and transiently expressed them in HeLa cells. mEos2-TRF1/2 specifically localized to telomeres (Figure 1B and S1A–B). Using photoactivated light microscopy (PALM) (Betzig et al., 2006), we determined the locations of telomere binding proteins with 15 nm precision in the *xy* plane (Movie S1) and 45 nm in the z direction (Movie S2). The dimensions of telomeric structures were calibrated by imaging mEos2-coated polystyrene beads under the same imaging conditions (Figure S1C). We observed that telomeres form compact structures smaller than the diffraction-limited resolution (~250 nm) of conventional microscopy (Figure 1B–C). Telomeric spots were nearly spherical, with an aspect ratio of ~0.78 ± 0.01 (mean ± SEM). The average number of mEos2-TRF2 molecules detected per telomere was 138 ± 10 (mean ± SEM) and the volume of telomeric chromatin was $2.3 \pm 0.2 \times 10^6$ nm^3 (mean ± SEM) (Figure 1D), in agreement with the size estimates based on immunogold labeling of telomeres (Luderus et al., 1996; Pierron and Puvion-Dutilleul, 1999).

To investigate how the size of telomeric structures changes as a function of telomere length, we performed PALM measurements in a HeLa subclone (HeLa 1.2.11), which has ~3.5 times longer telomeres (mean ~20 kb) than regular HeLa cells (~6 kb) (Takai et al., 2010). Telomere volume in HeLa 1.2.11 was 3.2-fold larger than in regular HeLa (Figure 1D). The DNA packing ratio of telomeric DNA was 5.4 ± 0.6 Mbp/μm^3 in regular HeLa and 4.9 ± 0.4 Mbp/μm^3 in HeLa 1.2.11 (Figure S1D, see Supplemental Experimental Procedures). The result demonstrates that longer telomeres form larger structures, but the DNA compaction ratio remains unaltered. We detected ~4 fold more TRF1/2 per telomere in HeLa 1.2.11 than regular HeLa (Figures 1D and S2A–B), consistent with estimates based on quantitative Western blots (Takai et al., 2010). In addition, telomeres with larger volume recruited more shelterin in HeLa cells (Pearson's r = 0.63, Figures 1E), suggesting that longer telomeric tracts form larger structures and recruit more shelterin (Smogorzewska et al., 2000).

To test whether telomere volume is affected by the expression of mEos2-tagged shelterin components, we directly labeled dsTEL tracts with an Alexa647-labeled peptide nucleic acid

(PNA) probe by fluorescence in situ hybridization (FISH) and measured telomere volume using stochastic optical reconstruction microscopy (STORM) (Rust et al., 2006) at 11 nm resolution (Figure S2C–D). Estimated volumes obtained from FISH-STORM imaging of telomeres in HeLa and HeLa 1.2.11 cells were slightly (15%) smaller than those based on PALM imaging of mEos2-TRF1. We concluded that our measurements are not markedly affected by the mEos2 fusions to shelterin, and that both protein and DNA components are equally compacted at telomeres.

To investigate whether telomere volume changes as a function of cell cycle, we synchronized HeLa cells at the G1/S boundary, mid-S, or in metaphase (Extended Experimental Procedures, Figure S1E). Cells synchronized at the G1/S boundary had telomere volumes similar (t-test, $p = 0.66$) to those of the unsynchronized cells (Figure 1F). Volume increased 1.8-fold (t-test, $p = 10^{-4}$) in mid-S phase, and decreased 20% (t-test $p = 0.08$) in the metaphase, compared to the G1/S boundary. The results suggest that telomeres partially decondense in S-phase during DNA replication, and then recompact post-replication. The average number of TRF2 localized to each telomere does not vary significantly throughout the cell-cycle (Figure 1G), in agreement with chromatin immunoprecipitation assays (Verdun et al., 2005).

It has been proposed that the hypercondensed structure of telomeric chromatin is a manifestation of DNA methylation, histone deacetylation and histone trimethylation at telomeres and subtelomeric regions (Schoeftner and Blasco, 2010). However, the interplay between the recruitment of these epigenetic marks and compaction of telomeric chromatin had not been directly measured. If these epigenetic marks determine the compact state of telomeres, their removal is expected to decondense chromatin globally and increase telomere volume. We treated HeLa cells with either a histone deacetylase inhibitor (trichostatin A [TSA]), a DNA methylation inhibitor (5-azacytidine [5-AZA]) or by knockdown of Suppressor of variegation (Suv) 39h1/2 and Suv4–20h1/2 involved in histone trimethylation. The analysis of both FISH-STORM and PALM measurements showed that telomere volume remains unaffected (t-test, $p > 0.3$) by these treatments compared to the untreated cells (Figures 1H and S1F). We conclude that DNA methylation, histone deacetylation and histone trimethylation are not primarily responsible for remodeling telomeres into a compact chromatin state.

Depletion of shelterin components leads to decompaction of telomeres

We next tested whether shelterin is primarily responsible for the crosslinking of dsTEL tracts through protein-protein interactions among different shelterin components (Figure 2A). To test this possibility, we measured the changes in telomere volume after individually depleting shelterin components in HeLa cells. TRF1, TIN2, TPP1, POT1 and RAP1 were depleted using RNA interference (RNAi) (Figure S3). Wild-type (WT) TRF2 was removed from telomeres by overexpressing a dominant negative mutant ($TRF2^{\Delta B \Delta M}$) (Doksani et al., 2013). Telomere volume was measured by FISH-STORM. Knockdown of RAP1 did not significantly affect the structure of telomeres (t-test, $p = 0.7$, Figure 2C and S4E), presumably because RAP1 interacts only with TRF2 and does not exhibit DNA remodeling activity. The depletion of TPP1 or POT1 resulted in a modest (~2-fold) increase in telomere

volume, whereas TIN2 depletion and the removal of TRF2 resulted in 6-fold and 5-fold increase in telomere volume, respectively (Figures 2B, 2C, S4A and S4E). TRF1 depletion resulted in 8-fold decompaction (Figures 2C and S4A). Simultaneous removal of TRF1 and TRF2, which is also expected to prevent TIN2 recruitment to telomeres, resulted in the largest (9-fold) increase in telomere volume (Figure 2C), corresponding to the DNA packing ratio of 0.7 ± 0.1 Mbp/μm^3. The DNA remodeling roles of TRF1 and TRF2 are likely not redundant, because the overexpression of TRF1 counteracts only 24% of telomere decompaction that is observed upon removal of TRF2 from telomeres in TRF2$^{\Delta B \Delta M}$ expressing cells (Figure S4C). Similar results (27%) were obtained when TRF2 was overexpressed in TRF1-depleted cells.

We also performed PALM imaging of telomeres using an mEos2-tagged MYB domain of TRF2 (TRF2^{MYB}) (Loayza and De Lange, 2003) and observed similar changes in volume upon depletion of shelterin subunits (Fig. S4C). The number of mEos2-tagged shelterin proteins detected per telomere strongly correlated with telomere volume (Pearson's r = 0.89) in these cells (Figures 2D and S4B), presumably due to the greater accessibility afforded by decompacted chromatin.

The results demonstrate that TRF1, TRF2 and TIN2 have the greatest impact on telomere compaction. To test whether interactions between these proteins compact telomeric chromatin, we expressed an mEos2-tagged TRF1 mutant (TRF1^{F142A}) that disrupts the TIN2-TRF1 interaction (Chen et al., 2008). The level of telomere decompaction was indistinguishable from TIN2-depleted cells expressing mEos2-TRF1 (t-test, p = 0.46, Figure S4D), suggesting that protein-protein interactions of the TRF1-TIN2-TRF2 ternary complex (Ye et al., 2004) facilitate telomere compaction.

Disruption of TRF1 and TRF2 dimerization results in telomere decompaction

TRF1 and TRF2 dimers contain two dsTEL binding sites that pair and loop telomeric tracts *in vitro* (Figure 3A) (Griffith et al., 1999). To test whether TRF dimerization plays a role in compacting telomeric chromatin *in vivo*, we disrupted the dimerization interface between the monomers by introducing single point mutations in helix 1 of the TRFH domains of TRF1 (A74D, A75P and F81P) and TRF2 (N53D and Y60F) (Figure 3B) (Fairall et al., 2001). Using size exclusion chromatography, we confirmed that the TRFH mutants of TRF1 are stable monomers, while TRF2 elutes as a weak dimer (Figure 3C).

Similarly to the removal of individual shelterin components from telomeres, expression of mEos2-tagged TRF1 and TRF2 dimerization mutants led to 3-fold and 5-fold increase in telomere volume, respectively (Figures 3D–E, S5A–B). The depletion of the endogenous TRF1/2 in these cells did not significantly affect the telomere volume, but increased the number of mEos2 spots localized per telomere by ~35% (Figure S5B–C). The cells expressing these mutants did not show a significant change in the cell-cycle distribution (Figure S5D).

Shelterin-mediated telomere compaction as a mechanism for telomere protection

Since chromatin structure plays a role in the initiation and propagation of DDR, we hypothesized that shelterin-mediated compaction of telomeric chromatin plays a major role in protecting telomeres against DDR signaling. To test this hypothesis, we simultaneously measured telomere volume and the accumulation of DDR signals (Sfeir and de Lange, 2012) at telomeres under various shelterin perturbation conditions. Telomere-dysfunction induced foci (TIF) per cell was quantified by the localization of p53 binding protein 1 (53BP1) (Figures 4A–B)(Karlseder et al., 1999; Shiloh, 2003), a downstream signaling protein recruited to DDR foci by both ATM and ATR pathways (Panier and Boulton, 2014). The TIF analysis provides a reliable measurement of the number of telomeres that recruit DDR signals, but does not discriminate among specific DDR pathways acting at telomeres.

We confirmed that removal of shelterin components leads to a large increase in TIF accumulation (Lackner et al., 2011). Cells expressing WT TRF1/2 had ~1–2 TIF spots per cell on average (Figure 4A). In comparison, TRF2, TRF1 and TIN2 depletion led to a 15 – 20 fold increase in the number of TIF spots per cell (Figures 4B–C, and S4F). We next tested whether the expression of TRFH mutants leads to TIF accumulation. The TRFH mutants localized well to telomeres (Figure S5C). The expression of TRFH mutants resulted in a 3–5 fold increase in the number of TIF spots per cell (Figures 4B–C, and S5E), demonstrating that TRFH dimerization is critical for telomere protection.

If shelterin-mediated telomere compaction is a mechanism to suppress DDR accumulation, we expect the cells to have a larger number of TIF spots as telomere volume increases. Consistent with this expectation, we observed that the number of TIF spots in these cells increases proportionally with telomere volume (Figure 4C, Pearson's $r = 0.82$). The results suggest that shelterin components remodel telomeric chromatin into a compact form and prevent access of DDR signals to telomeric sites. To verify that the results are not specific to transformed cells, we expressed WT and the N53D mutant of TRF2 in IMR-90 human fibroblasts. Similar to our observations in HeLa cells, TRF2-N53D expression resulted in 3 fold increase telomere volume and 9-fold increase in TIF spots per cell, in comparison to WT TRF2 expressing cells (Figure S5F–H).

On the basis of these results, we propose that shelterin condenses telomeric repeats into a dense network of nucleoprotein structures, resulting in a tight globular mesh. Removal of shelterin components or weakening of these interactions leads to the decompaction of condensed telomeric structures and enables access of DDR signaling proteins to telomeres (Figure 5A). To test this prediction, we measured the average accessibility of soluble shelterin components to both the surface and interior of telomeric chromatin using fluorescence recovery after photobleaching (FRAP) (Figure 5B and S6A). Consistent with a previous report (Mattern et al., 2004), GFP-fusions of TRF1, TRF2 and POT1 dynamically interacted with telomeres. Remarkably, the fluorescence recovery lifetime (τ) of GFP-POT1 at telomeres in TRF1-depleted cells (11.5 ± 0.7 s; mean ± SEM) was approximately one half that of untreated cells (20.6 ± 1.1 s) (Figure 5B–C, Movie S3) and the fraction of mobile molecules increased from 0.60 to 0.73.

Additionally, τ of TRF2-N53D (10.1 ± 0.6 s) and TRF2-Y60F (11.0 ± 0.5 s) were significantly shorter than that of WT-TRF2 (17.7 ± 1.6 s) and the fraction of mobile molecules increased from 0.65 to 0.85 (Figures 5D and S6A, Movie S4). An increase in both exchange rate and abundance of the mobile fraction of the shelterin components upon telomere decompaction is consistent with our prediction that DNA decompaction increases the accessibility of telomere-interacting proteins to the interior of telomeric chromatin. Observed recovery in compact telomeric structures is most likely due to protein exchange with the surface of telomeric chromatin.

Shelterin-mediated telomere decompaction is independent of DDR accumulation

In principle, the results presented above are also consistent with the possibility that activation of the DDR at telomeres leads to DNA decompaction, rather than *vice versa* (Figure 6A). To distinguish whether DNA decompaction or DDR accumulation occurs first at telomeres upon loss of shelterin components, we specifically triggered the non-homologous end joining (NHEJ) pathway at telomeres by expressing $TRF2^{MYB}$ or $TRF2^{\Delta B\Delta M}$ (Karlseder et al., 1999). If DDR accumulation, not shelterin removal, leads to telomere decompaction, removal of endogenous TRF2 from telomeres by $TRF2^{MYB}$ or $TRF2^{\Delta B\Delta M}$ expression is not expected to exhibit telomere decompaction in ATM-inactive cells. To inactivate the NHEJ pathway, we depleted ATM kinase, MRE11A or Ku70 in HeLa cells using RNAi (Figure S3C)(Lottersberger et al., 2013). Expression of $TRF2^{MYB}$ in ATM kinase depleted cells did not result in a significant increase in the number of TIF spots (Figures 6B–C, $p = 0.49$), demonstrating that these cells are incapable of activating the ATM pathway. Similar to untreated cells, expression of $TRF2^{MYB}$ in cells depleted of ATM kinase, MRE11A or Ku70 led to ~2–4-fold increase in telomere volume (Figures 6D and S6B). In addition, depletion of ATM kinase did not significantly affect decompaction of telomeric chromatin in $TRF2^{\Delta B\Delta M}$ expressing cells (Figure S6C).

The recruitment of DDR proteins led to a further 20–40% DNA decompaction (Wilcoxon Rank test, $p = 0.0005$, Figure S6D), in agreement with the decompaction of nontelomeric regions following activation of DDR signals (Floyd et al., 2013). Alternatively, ATM-mediated TRF1 phosphorylation has been shown to down-regulate TRF1 association with telomeres (Kishi and Lu, 2002; Wu et al., 2007), which would lead to decompaction. Importantly, the 20–40% increase in telomere volume by DDR accumulation is relatively minor compared to the 5–10 fold decompaction upon TRF1, TRF2 or TIN2 removal. Therefore, the decompaction of telomeric chromatin is mainly due to the removal of or mutations to shelterin components, not the result of DDR accumulation.

Reversible control of telomere compaction alters TIF accumulation

The strong correlation we observed between telomere decompaction and TIF accumulation could also arise if these were two independent processes that occur simultaneously when shelterin components are inactivated or depleted (Figure 7A). If this were the case, the recompaction of telomeric chromatin would not be expected to rescue telomeres against TIF accumulation (Figure 7A, blue and red arrows). To test this idea, we developed an orthogonal method to recompact telomeres following perturbations of shelterin components.

First, we tested the role of TRF2 dimerization in telomere protection while maintaining other telomere-related functions of TRF2. Because TRF2 dimerization mutants tightly bind to telomeres (Figure 3D), they are expected to retain their interactions with telomere-associated proteins in the monomeric state. The N-terminus of a TRF2 dimerization mutant (N53D and Y60F) was fused to a DmrB tag, which undergoes chemically-inducible dimerization in the presence of a BB dimerizer (Figure 7B). Expression of DmrB-TRF2-N53D in the absence of BB led to telomere decompaction and TIF accumulation (Figures 7C–D and S7), similar to that observed in cells expressing untagged versions of these mutants (Figures 3E and 4B). Addition of BB induced compaction of telomeric chromatin comparable to that of native cells. Washing out BB with a competing ligand led to a similar increase in telomere volume, as was observed in the absence of BB. Finally, addition of BB after the removal of the competing ligand rescued telomere compaction. Therefore, telomeres were reversibly decompacted and recompacted by controlling the monomer-to-dimer formation of DmrB-TRF2-N53D (Figure 7C, 7D). Contrary to the prediction of the model in Figure 7A, the number of TIF spots per cell strongly correlated (Pearson's r = 0.91) with the changes in telomere volume, providing a mechanistic link between chromatin decompaction and DDR activation at telomeres. Similar results were observed with DmrB-TRF2-Y60F (Figure S7). These results are also consistent with the reversibility of telomere deprotection using a temperature-sensitive mutant of TRF2 (Konishi and de Lange, 2008).

To further demonstrate that recompaction of telomeric chromatin removes DDR signals from telomeres, we attempted to recompact telomeric chromatin in TIN2-depleted cells. Unlike the rescue of TRF2 dimerization, integrity of the shelterin complex could not be maintained in these cells, because TRF1, TRF2 and TPP1 do not interact with each other in the absence of TIN2. We tested whether the lack of TIN2 can be compensated by overexpression of TRF1 or TRF2, which compact telomeric chromatin by a mechanism fundamentally distinct from that of TIN2. Consistent with our model, TRF2 overexpression rescued telomere decompaction by ~31% and reduced the number of TIFs by 53% (Fig 7E). Remarkably, TRF1 overexpression compensated for the removal of TIN2 from telomeres by 85% in both telomere decompaction and TIF accumulation, in agreement with its major role in telomere remodeling. Together, these results demonstrate that shelterin-mediated telomere compaction significantly reduces TIF accumulation.

DISCUSSION

In this study, we directly observed that human telomeres are condensed into tight globular structures *in vivo*, similar to those seen in mouse cells (Doksani et al., 2013). Hypercondensation of telomeres is primarily mediated by shelterin components and telomeric DNA, not by histone deacetylation, DNA methylation or histone trimethylation. We have provided evidence that shelterin-mediated telomere compaction plays a major role in the protection of mammalian telomeres from targeting by the DDR machinery. Removal or manipulation of shelterin components leads to decompaction of telomeric chromatin, which triggers access of DDR signals at telomere ends. These results challenge the established views of how cells solve the chromosome end-capping problem. We propose that shelterin components safeguard telomere ends not only by binding to the telomeric sites that are prone to DDR recognition, but also by remodeling telomeric DNA into a dense

network of nucleoprotein structures, which substantially reduce the accessibility of DDR signals.

Shelterin mediates high-order compaction of telomeric chromatin

Shelterin compacts telomeric DNA primarily through the action of TIN2, which bridges TRF1 and TRF2 bound to distal dsTEL tracts. Because each TRF1 and TRF2 homodimer can potentially interact with two TIN2 molecules, telomeric chromatin may be crosslinked extensively through a complex network of interactions between shelterin and telomeric DNA. Mutations that disrupt TRF1 or TRF2 homodimerization, but not their localization to telomeres, also led to an increase in telomere volume, consistent with the ability of these proteins to loop (Griffith et al., 1998; Griffith et al., 1999) and condense (Poulet et al., 2012) telomeric tracts *in vitro*. Depletion of TRF1 and TRF2 leads to higher levels of telomere decompaction than expression of their dimerization mutants, presumably because depletion impairs both mechanisms of inter-repeat crosslinking.

Remarkably, disrupting TRF2 dimerization resulted in a larger increase in telomere volume than that of TRF1, in contrast to larger decompaction observed in TRF1 depleted cells compared to the TRF2 removal (Figure 2B), suggesting that TRF1 and TRF2 play distinct DNA remodeling roles during telomere compaction. TRF1 recruitment may be more critical for the assembly of shelterin onto telomeres and for the crosslinking of dsTEL tracts. TRF2 preferentially binds to three- and four-way junctions (Fouche et al., 2006; Poulet et al., 2009) and facilitates t-loop formation (Griffith et al., 1999), which may require TRF2 dimerization.

The Telomere Compaction Model

The removal or perturbation of shelterin components resulted in a large increase in telomere volume. Decompacted telomeres were more likely to recruit DDR signals, suggesting that DNA compaction reduces the access of DDR signals to telomeres. The model is consistent with the view that euchromatin, which is less compact, exhibits faster detection and repair kinetics as compared to heterochromatin (Murga et al., 2007). Accessibility differences could result from differential compaction levels such that ssTEL and dsTEL tracts buried inside a compact mesh are shielded from the DDR signals. Alternatively, DDR components may access telomeres due to loss of selective permeability (Lenart et al., 2003) or phase separation (Li et al., 2012) upon the removal of shelterin components.

It has been shown that depletion of individual shelterin components triggers specific DDR pathways at ssTEL tracts or the ssTEL/dsTEL junction (Sfeir and de Lange, 2012). The telomere compaction mechanism is consistent with these observations and suggests that shelterin has at least two major roles in telomere capping and DDR suppression. First, shelterin condenses telomeric repeats into a dense network of nucleoprotein structures and reduces the accessibility of the sites that are prone to DDR recognition. Thus, shelterin-mediated chromatin compaction serves as a general mechanism for protection against a wide variety of DDR pathways at telomeres. Second, TRF2 and POT1 tightly bind to dsTEL/ssTEL junction and ssTEL tracts (Palm and de Lange, 2008) and specifically suppress the

initiation of ATM and ATR pathways, respectively. Therefore, removal of these proteins from telomeres leads to the activation of specific DDR pathways.

Efficient protection of telomeres is likely to require both the compaction of telomeric chromatin and the binding of individual shelterin components to ssTEL tracts or the ssTEL/dsTEL junction. When the interactions between shelterin components are compromised, telomeric chromatin decompacts and the protected telomeric sites become accessible to DDR proteins. As a result, DDR signaling proteins more effectively displace shelterin components from ssTEL tracts or the ssTEL/dsTEL junction.

TIN2 is essential for efficient protection of telomeres against both ATM and ATR (Sfeir and de Lange, 2012; Takai et al., 2011), although TIN2 does not directly bind to telomeric DNA. Our model predicts that TIN2 compacts telomeric chromatin by interacting simultaneously with TRF1 and TRF2 (Takai et al., 2011), effectively reducing the accessibility of telomeres to DDR signals. Furthermore, TIN2 stabilizes the interaction of POT1/TPP1 with ssTEL by crosslinking it to the rest of the shelterin complex (Takai et al., 2011), thus reducing the ability of RPA to displace POT1 from ssTEL. Consistently, a TIN2 mutant that does not interact with TRF1 triggers ATM, ATR and classical NHEJ pathways, but protection against all three pathways was restored when the mutant was artificially linked to RAP1 (Frescas and de Lange, 2014). This could be because the artificial TIN2-RAP1 link reestablishes the complex network of interactions for the compaction of telomeric chromatin.

The telomere compaction model is not mutually exclusive with the proposed roles of t-loops in DDR prevention (Palm and de Lange, 2008). T-loops were not visible in super-resolution images, probably due to the elasticity and high-order compaction of telomeric DNA.

Implications for Telomere Length Control

The telomere compaction mechanism may also have important implications for telomere length control. Telomeres gradually shorten during each cell division, and telomere attrition is counteracted by telomerase, a reverse transcriptase that adds telomeric repeats at the terminus of the G-overhang (Egan and Collins, 2012). Short telomeres serve as a better substrate for telomerase than long telomeres, creating a feedback mechanism to maintain the telomere length (Takai et al., 2010). The protein counting model proposed that longer telomeres recruit more TRF1 and TRF2, and form a closed state that inhibits telomerase access (Smogorzewska et al., 2000). As telomeres gradually shorten, they switch to an open state due to the scarcity of TRF1 and TRF2. Our results are consistent with this model and provide a structural basis for the open and closed states of telomeres. The closed state may correspond to the shelterin-mediated compaction of telomeric chromatin, which may block the access of telomerase to the G-overhang, in a manner similar to the suppression of the DDR signals. Telomeres may switch to an open state as they shorten due to the inability of short telomeres to form compact chromatin structures. Alternatively, the G-overhang becomes permeable or surface-exposed in short telomeres, and recruits telomerase to its terminus.

In addition to their DNA binding and remodeling roles, shelterin components recruit accessory factors that reduce access of upstream DDR signals to telomeres (Okamoto et al.,

2013), and directly interact with histone proteins (Galati et al., 2006; Pisano et al., 2010), telomeric repeat-containing RNA (Deng et al., 2009) and telomerase (Nandakumar et al., 2012; Sexton et al., 2012). We anticipate that the experimental approach developed in this study will serve as a powerful tool to map out how shelterin and other telomere associated factors contribute to higher-order remodeling and maintenance of telomeric chromatin *in vivo*.

EXPERIMENTAL PROCEDURES

Cloning, Protein Expression and Purification

TRFH point mutants of TRF1 and TRF2 were expressed in *E. coli*. Size exclusion chromatography was performed using a HiLoad 16/600 Superdex 200 pg column. For PALM imaging assays, native and mutant human shelterin components were cloned into the pEGFP-C1 vector containing an N-terminal mEos2. TRF2$^{\Delta B \Delta M}$ was fused to BFP for multicolor PALM imaging. For telomere rescue assays, a DmrB tag (Clontech) was fused to the N-terminus of TRF2-N53D and TRF2-Y60F. The complete list of plasmids used is shown in Table S1.

Cell Culture

Human cells were cultured at 37°C. Transfections were performed using Lipofectamine 2000 at 50–70% confluence. 24–48 hours post-transfection, the cells were fixed with 4% paraformaldehyde. For cell-cycle measurements, HeLa cells were synchronized with a double thymidine block. Cell cycle distribution of the cells was quantified by flow cytometry. siRNA and shRNA mediated depletion of telomere associated proteins were determined by real-time PCR and fluorescence imaging.

Imaging and Data Analysis

Images for TIF analysis were collected using confocal microscopy. FRAP measurements were performed on a Zeiss LSM 710 microscope. Telomeres were photobleached using 0.8 mW focused 488 nm beam and fluorescence recovery at telomeres was measured every 3 s under 0.4 μW excitation.

FISH samples were prepared as described (Lackner et al., 2011). STORM imaging was done in PBS buffer supplemented with methylethylamine (MEA) and protocatechuic acid/ protocatechuate-3,4-dioxygenase (PCA/PCD) system.

Superresolution images were recorded using a cycle containing one frame for photoconversion at 405 nm excitation followed by 5 frames of imaging under 532 nm excitation (150 ms per frame). Camera acquisition and laser excitation were synchronized through custom software written in LabView. Images were analyzed using software provided by B. Huang (UCSF). The resolution of 2D PALM imaging is defined as SEM of a typical mEos2 spot.

Detailed procedures for cloning, purification, light microscopy and data analysis are described in Extended Experimental Procedures.

Supplementary Material

Refer to Web version on PubMed Central for supplementary material.

Acknowledgments

We thank K. Collins, A. Dernburg and G. Karpen for critically reading our manuscript, B. Huang for the data analysis software, M. Lei and J. Nandakumar for shelterin plasmids, T. de Lange for HeLa 1.2.11 cells, E. Griffis for advice in transfections and J. Canty for help with superresolution imaging. This work has been supported by NIH (GM094522 to A.Y.), NSF (MCB-1055017 to A.Y.) and Ellison Medical Foundation (A.Y.).

References

Benetti R, Garcia-Cao M, Blasco MA. Telomere length regulates the epigenetic status of mammalian telomeres and subtelomeres. Nature genetics. 2007; 39:243–250. [PubMed: 17237781]

Betzig E, Patterson GH, Sougrat R, Lindwasser OW, Olenych S, Bonifacino JS, Davidson MW, Lippincott-Schwartz J, Hess HF. Imaging intracellular fluorescent proteins at nanometer resolution. Science. 2006; 313:1642–1645. [PubMed: 16902090]

Blasco MA. Telomeres as therapeutic targets for cancer and aging. Hum Gene Ther. 2013; 24:A19–A19.

Cacchione S, Cerone MA, Savino M. In vitro low propensity to form nucleosomes of four telomeric sequences. FEBS letters. 1997; 400:37–41. [PubMed: 9000509]

Chen Y, Yang YT, van Overbeek M, Donigian JR, Baciu P, de Lange T, Lei M. A shared docking motif in TRF1 and TRF2 used for differential recruitment of telomeric proteins. Science. 2008; 319:1092–1096. [PubMed: 18202258]

Deng Z, Norseen J, Wiedmer A, Riethman H, Lieberman PM. TERRA RNA Binding to TRF2 Facilitates Heterochromatin Formation and ORC Recruitment at Telomeres. Molecular cell. 2009; 35:403–413. [PubMed: 19716786]

Doksani Y, Wu JY, de Lange T, Zhuang X. Super-Resolution Fluorescence Imaging of Telomeres Reveals TRF2-Dependent T-loop Formation. Cell. 2013; 155:345–356. [PubMed: 24120135]

Egan ED, Collins K. Biogenesis of telomerase ribonucleoproteins. Rna. 2012; 18:1747–1759. [PubMed: 22875809]

Fairall L, Chapman L, Moss H, De Lange T, Rhodes D. Structure of the TRFH dimerization domain of the human telomeric proteins TRF1 and TRF2. Molecular cell. 2001; 8:351–361. [PubMed: 11545737]

Floyd SR, Pacold ME, Huang QY, Clarke SM, Lam FC, Cannell IG, Bryson BD, Rameseder J, Lee MJ, Blake EJ, et al. The bromodomain protein Brd4 insulates chromatin from DNA damage signalling. Nature. 2013; 498:246. [PubMed: 23728299]

Fouche N, Cesare AJ, Willcox S, Ozgur S, Compton SA, Griffith JD. The basic domain of TRF2 directs binding to DNA junctions irrespective of the presence of TTAGGG repeats. Journal of Biological Chemistry. 2006; 281:37486–37495. [PubMed: 17052985]

Frescas D, de Lange T. TRF2-Tethered TIN2 Can Mediate Telomere Protection by TPP1/POT1. Molecular and cellular biology. 2014; 34:1349–1362. [PubMed: 24469404]

Galati A, Magdinier F, Colasanti V, Bauwens S, Pinte S, Ricordy R, Giraud-Panis MJ, Pusch MC, Savino M, Cacchione S, et al. TRF2 Controls Telomeric Nucleosome Organization in a Cell Cycle Phase-Dependent Manner. Plos One. 2012; 7

Galati A, Rossetti L, Pisano S, Chapman L, Rhodes D, Savino M, Cacchione S. The human telomeric protein TRF1 specifically recognizes nucleosomal binding sites and alters nucleosome structure. J Mol Biol. 2006; 360:377–385. [PubMed: 16756990]

Griffith J, Bianchi A, de Lange T. TRF1 promotes parallel pairing of telomeric tracts in vitro. J Mol Biol. 1998; 278:79–88. [PubMed: 9571035]

Griffith JD, Comeau L, Rosenfield S, Stansel RM, Bianchi A, Moss H, de Lange T. Mammalian telomeres end in a large duplex loop. Cell. 1999; 97:503–514. [PubMed: 10338214]

Herbig U, Jobling WA, Chen BPC, Chen DJ, Sedivy JM. Telomere shortening triggers senescence of human cells through a pathway involving ATM, p53, and p21(CIP1), but not p16(INK4a). Molecular cell. 2004; 14:501–513. [PubMed: 15149599]

Ichikawa Y, Morohashi N, Nishimura Y, Kurumizaka H, Shimizu M. Telomeric repeats act as nucleosome-disfavouring sequences in vivo. Nucleic acids research. 2014; 42:1541–1552. [PubMed: 24174540]

Karlseder J, Broccoli D, Dai Y, Hardy S, de Lange T. p53-and ATM-dependent apoptosis induced by telomeres lacking TRF2. Science. 1999; 283:1321–1325. [PubMed: 10037601]

Karlseder J, Hoke K, Mirzoeva OK, Bakkenist C, Kastan MB, Petrini JH, de Lange T. The telomeric protein TRF2 binds the ATM kinase and can inhibit the ATM-dependent DNA damage response. PLoS biology. 2004; 2:E240. [PubMed: 15314656]

Kishi S, Lu KP. A critical role for Pin2/TRF1 in ATM-dependent regulation. Inhibition of Pin2/TRF1 function complements telomere shortening, radiosensitivity, and the G(2)/M checkpoint defect of ataxia-telangiectasia cells. J Biol Chem. 2002; 277:7420–7429. [PubMed: 11744712]

Konishi A, de Lange T. Cell cycle control of telomere protection and NHEJ revealed by a ts mutation in the DNA-binding domain of TRF2. Genes Dev. 2008; 22:1221–1230. [PubMed: 18451109]

Lackner DH, Durocher D, Karlseder J. A siRNA-Based Screen for Genes Involved in Chromosome End Protection. Plos One. 2011; 6

Lenart P, Rabut G, Daigle N, Hand AR, Terasaki M, Ellenberg J. Nuclear envelope breakdown in starfish oocytes proceeds by partial NPC disassembly followed by a rapidly spreading fenestration of nuclear membranes. J Cell Biol. 2003; 160:1055–1068. [PubMed: 12654902]

Li P, Banjade S, Cheng HC, Kim S, Chen B, Guo L, Llaguno M, Hollingsworth JV, King DS, Banani SF, et al. Phase transitions in the assembly of multivalent signalling proteins. Nature. 2012; 483:336–340. [PubMed: 22398450]

Liu D, Safari A, O'Connor MS, Chan DW, Laegeler A, Qin J, Songyang Z. PTOP interacts with POT1 and regulates its localization to telomeres. Nature cell biology. 2004; 6:673–680. [PubMed: 15181449]

Loayza D, De Lange T. POT1 as a terminal transducer of TRF1 telomere length control. Nature. 2003; 423:1013–1018. [PubMed: 12768206]

Lorat Y, Schanz S, Schuler N, Wennemuth G, Rube C, Rube CE. Beyond Repair Foci: DNA Double-Strand Break Repair in Euchromatic and Heterochromatic Compartments Analyzed by Transmission Electron Microscopy. Plos One. 2012; 7

Lottersberger F, Bothmer A, Robbiani DF, Nussenzweig MC, de Lange T. Role of 53BP1 oligomerization in regulating double-strand break repair. Proceedings of the National Academy of Sciences of the United States of America. 2013; 110:2146–2151. [PubMed: 23345425]

Luderus ME, vanSteensel B, Chong L, Sibon OCM, Cremers FFM, deLange T. Structure, subnuclear distribution, and nuclear matrix association of the mammalian telomeric complex. J Cell Biol. 1996; 135:867–881. [PubMed: 8922373]

Martinez P, Thanasoula M, Munoz P, Liao CY, Tejera A, McNees C, Flores JM, Fernandez-Capetillo O, Tarsounas M, Blasco MA. Increased telomere fragility and fusions resulting from TRF1 deficiency lead to degenerative pathologies and increased cancer in mice. Genes & development. 2009; 23:2060–2075. [PubMed: 19679647]

Mattern KA, Swiggers SJJ, Nigg AL, Lowenberg B, Houtsmuller AB, Zijlmans JMJM. Dynamics of protein binding to telomeres in living cells: Implications for telomere structure and function. Molecular and cellular biology. 2004; 24:5587–5594. [PubMed: 15169917]

McKinney SA, Murphy CS, Hazelwood KL, Davidson MW, Looger LL. A bright and photostable photoconvertible fluorescent protein. Nat Chem Biol. 2009; 6:131–133.

Munoz-Jordan JL, Cross GAM, de Lange T, Griffith JD. T-loops at trypanosome telomeres. Embo Journal. 2001; 20:579–588. [PubMed: 11157764]

Murga M, Jaco I, Fan Y, Soria R, Martinez-Pastor B, Cuadrado M, Yang SM, Blasco MA, Skoultchi AI, Fernandez-Capetillo O. Global chromatin compaction limits the strength of the DNA damage response. J Cell Biol. 2007; 178:1101–1108. [PubMed: 17893239]

Nagano T, Lubling Y, Stevens TJ, Schoenfelder S, Yaffe E, Dean W, Laue ED, Tanay A, Fraser P. Single-cell Hi-C reveals cell-to-cell variability in chromosome structure. Nature. 2013; 502:59–64. [PubMed: 24067610]

Nandakumar J, Bell CF, Weidenfeld I, Zaug AJ, Leinwand LA, Cech TR. The TEL patch of telomere protein TPP1 mediates telomerase recruitment and processivity. Nature. 2012; 492:285–289. [PubMed: 23103865]

O'Connor MS, Safari A, Xin HW, Liu D, Songyang Z. A critical role for TPP1 and TIN2 interaction in high-order telomeric complex assembly. Proceedings of the National Academy of Sciences of the United States of America. 2006; 103:11874–11879. [PubMed: 16880378]

Okamoto K, Bartocci C, Ouzounov I, Diedrich JK, Yates JR 3rd, Denchi EL. A two-step mechanism for TRF2-mediated chromosome-end protection. Nature. 2013; 494:502–505. [PubMed: 23389450]

Palm W, de Lange T. How Shelterin Protects Mammalian Telomeres. Annu Rev Genet. 2008; 42:301–334. [PubMed: 18680434]

Panier S, Boulton SJ. Double-strand break repair: 53BP1 comes into focus. Nat Rev Mol Cell Bio. 2014; 15:7–18. [PubMed: 24326623]

Pierron G, Puvion-Dutilleul F. An anchorage nuclear structure for telomeric DNA repeats in HeLa cells. Chromosome Res. 1999; 7:581–592. [PubMed: 10628659]

Pisano S, Leoni D, Galati A, Rhodes D, Savino M, Cacchione S. The human telomeric protein hTRF1 induces telomere-specific nucleosome mobility. Nucleic acids research. 2010; 38:2247–2255. [PubMed: 20056655]

Pisano S, Marchioni E, Galati A, Mechelli R, Savino M, Cacchione S. Telomeric nucleosomes are intrinsically mobile. J Mol Biol. 2007; 369:1153–1162. [PubMed: 17498745]

Poulet A, Buisson R, Faivre-Moskalenko C, Koelblen M, Amiard S, Montel F, Cuesta-Lopez S, Bornet O, Guerlesquin F, Godet T, et al. TRF2 promotes, remodels and protects telomeric Holliday junctions. Embo Journal. 2009; 28:641–651. [PubMed: 19197240]

Poulet A, Pisano S, Faivre-Moskalenko C, Pei B, Tauran Y, Haftek-Terreau Z, Brunet F, Le Bihan YV, Ledu MH, Montel F, et al. The N-terminal domains of TRF1 and TRF2 regulate their ability to condense telomeric DNA. Nucleic acids research. 2012; 40:2566–2576. [PubMed: 22139926]

Rust MJ, Bates M, Zhuang X. Sub-diffraction-limit imaging by stochastic optical reconstruction microscopy (STORM). Nat Methods. 2006; 3:793–795. [PubMed: 16896339]

Schoeftner S, Blasco MA. Chromatin regulation and non-coding RNAs at mammalian telomeres. Semin Cell Dev Biol. 2010; 21:186–193. [PubMed: 19815087]

Sexton AN, Youmans DT, Collins K. Specificity Requirements for Human Telomere Protein Interaction with Telomerase Holoenzyme. Journal of Biological Chemistry. 2012; 287:34455–34464. [PubMed: 22893708]

Sfeir A, de Lange T. Removal of Shelterin Reveals the Telomere End-Protection Problem. Science. 2012; 336:593–597. [PubMed: 22556254]

Sfeir A, Kabir S, van Overbeek M, Celli GB, de Lange T. Loss of Rap1 induces telomere recombination in the absence of NHEJ or a DNA damage signal. Science. 2010; 327:1657–1661. [PubMed: 20339076]

Shiloh Y. ATM and related protein kinases: Safeguarding genome integrity. Nat Rev Cancer. 2003; 3:155–168. [PubMed: 12612651]

Smogorzewska A, van Steensel B, Bianchi A, Oelmann S, Schaefer MR, Schnapp G, de Lange T. Control of human telomere length by TRF1 and TRF2. Molecular and cellular biology. 2000; 20:1659–1668. [PubMed: 10669743]

Takai KK, Hooper S, Blackwood S, Gandhi R, de Lange T. In vivo stoichiometry of shelterin components. Journal of Biological Chemistry. 2010; 285:1457–1467. [PubMed: 19864690]

Takai KK, Kibe T, Donigian JR, Frescas D, de Lange T. Telomere Protection by TPP1/POT1 Requires Tethering to TIN2. Molecular cell. 2011; 44:647–659. [PubMed: 22099311]

Verdun RE, Crabbe L, Haggblom C, Karlseder J. Functional human telomeres are recognized as DNA damage in G2 of the cell cycle. Molecular cell. 2005; 20:551–561. [PubMed: 16307919]

Wu Y, Xiao S, Zhu XD. MRE11-RAD50-NBS1 and ATM function as comediators of TRF1 in telomere length control. Nat Struct Mol Biol. 2007; 14:832–840. [PubMed: 17694070]

Ye JZS, Donigian JR, van Overbeek M, Loayza D, Luo Y, Krutchinsky AN, Chait BT, de Lange T. TIN2 binds TRF1 and TRF2 simultaneously and stabilizes the TRF2 complex on telomeres. The Journal of biological chemistry. 2004; 279:47264–47271. [PubMed: 15316005]

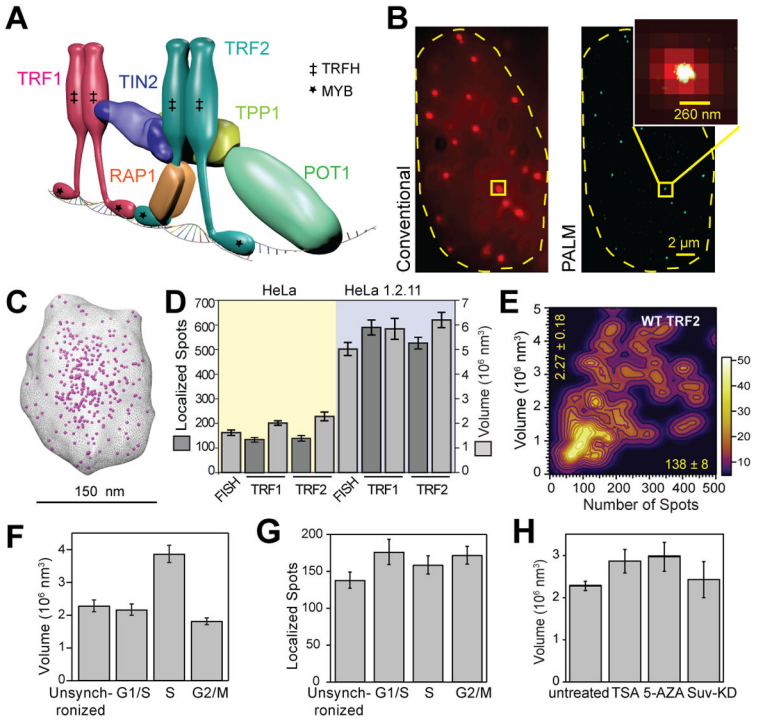

Figure 1. Human telomeres form tight globular structures

(A) The human shelterin complex consists of six proteins: TRF1, TRF2, POT1, TPP1, TIN2 and RAP1. TRF1 and TRF2 subunits specifically bind to dsTEL tracts through their C-terminal MYB domains and homodimerize via their N-terminal TRFH domains.

(B) Conventional (left) and PALM (right) images of a HeLa cell expressing mEos2-TRF2. TRF2 proteins are localized to nucleus (yellow boundary) and show punctate spots that represent telomeres. Telomeric chromatin appears smaller than a diffraction-limited spot (insert).

(C) 3D representation of a telomeric chromatin constructed from individual spots (magenta dots).

(D) The average volume and the number of localized spots detected per telomere in regular HeLa and HeLa 1.2.11 cells. Error bars represent SEM. $N_{telomeres}$ is >150 for each case.

(E) The volume of telomeric structures in mEos2-TRF2 expressing cells positively correlates with the number of detected TRF2 molecules per telomeres ($N_{telomeres}$ >150). Color bar shows the number of telomeres (mean ± SEM).

(F) The average volume of telomeres in G1/S phase is similar to that of unsynchronized cells.

(G) The average number of TRF2 molecules detected per telomere remains similar in different stages of the cell cycle.

(H) The volume of telomeres in mEos2-TRF2 expressing cells remains unaffected by inhibition of histone deacetylation, DNA methylation and Suv knockdown.

See also Figures S1 and S2, Movies S1 and S2.

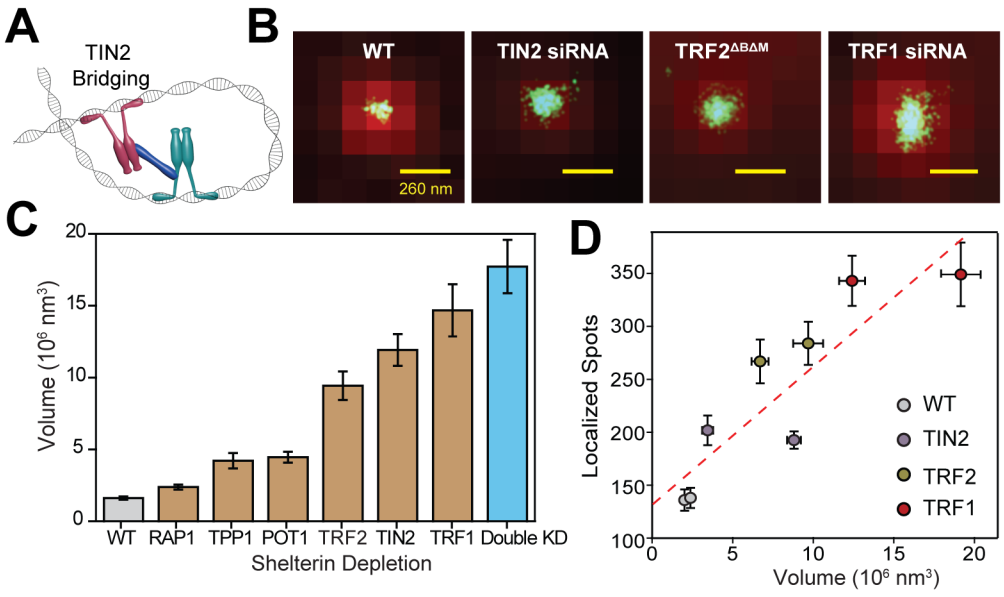

Figure 2. Removal of shelterin subunits leads to decompaction of telomeres

(A) A schematic represents the looping of dsTEL tracts by TIN2, which bridges dsTEL-bound TRF1 and TRF2.

(B) Representative FISH-STORM images of telomeres in WT and TRF1, TRF2 and TIN2 depleted cells.

(C) The average volume of telomeres in WT and shelterin-depleted cells measured by FISH-STORM (N >150 per condition). Error bars represent SEM.

(D) In PALM imaging, the average number of mEos2 spots localized to each telomere correlated with the average volume of the telomere under native and shelterin knockdown (KD) conditions (dotted line, Pearson's r = 0.89). Error bars represent SEM.

See also Figures S3 and S4.

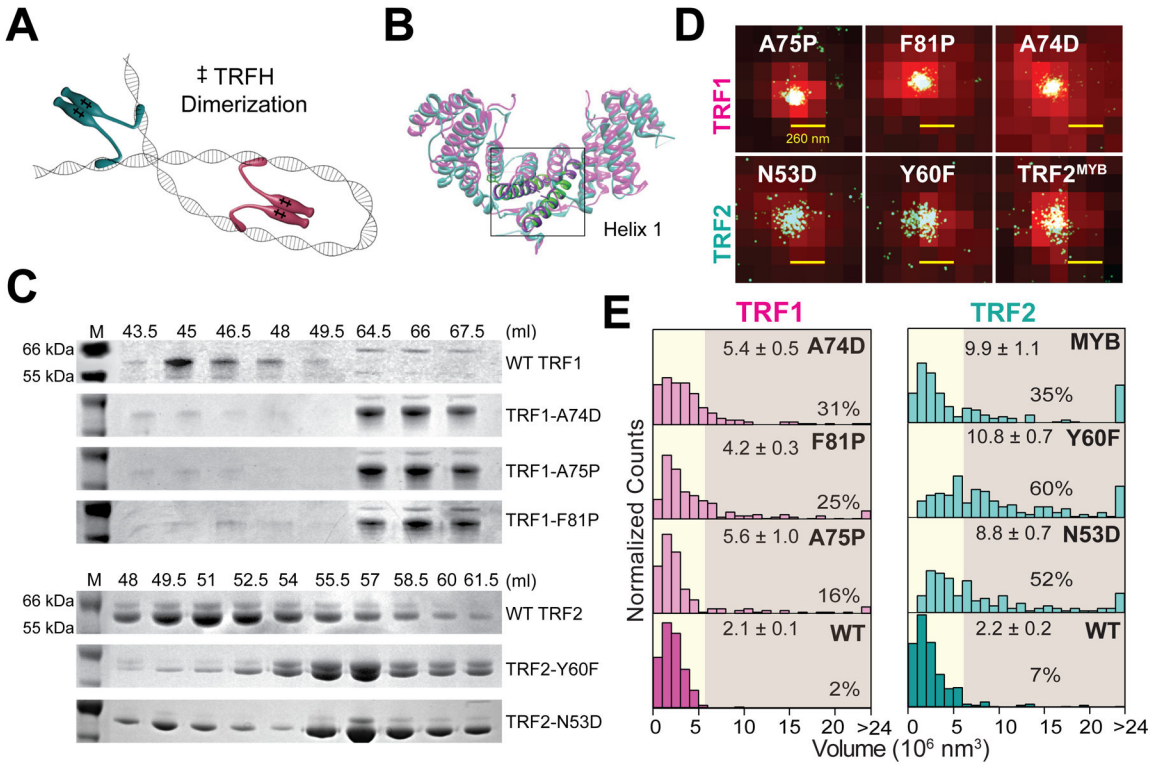

Figure 3. TRF1 and TRF2 dimerization is essential for the compaction of telomeres

(A) A schematic depicting the crosslinking of distal dsTEL tracts through TRF1 or TRF2 homodimerization.

(B) Overlay of the atomic structures of the TRFH domains of TRF1 (magenta) and TRF2 (cyan-green) dimers. Single–point mutations were introduced to helix 1 to disrupt dimerization.

(C) Gel filtration profiles show that WT TRF1 and TRF2 elute as homodimers, whereas TRFH point mutations elute as monomers.

(D) Representative telomeric structures for TRF1 and TRF2 dimerization mutants.

(E) The distribution of telomere volume in cells expressing the TRFH mutants ($N_{telomeres}$ >150). The expression of the TRFH mutants increases the average volume of telomeres (mean ± SEM). Percentages represent the data in pink shaded regions.

See also Figure S5.

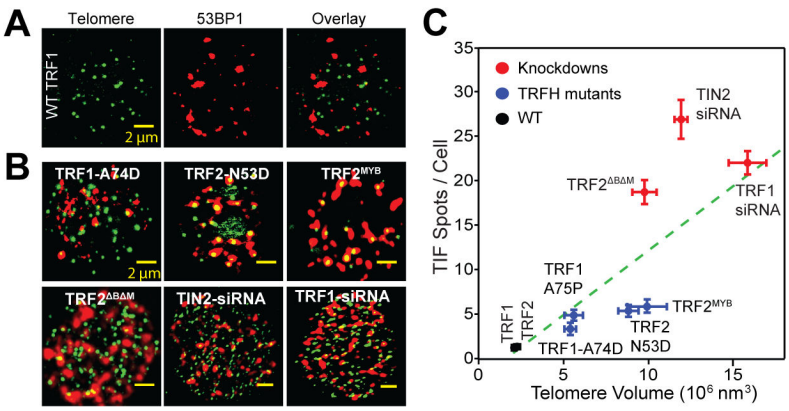

Figure 4. Decompaction of telomeres correlates with the number of TIF spots per cell

(A) Telomeres were detected using Alexa-488-labeled antibodies against TRF1 or TRF2 (green) and DNA repair sites were probed by immunolabeling of 53BP1 with Alexa-647 (red). The overlay reveals the location of TIF spots (yellow).

(B) The knockdown of shelterin components and the expression of TRFH dimerization mutants induce localization of DDR signals at telomeres. TIF spots (yellow) were determined by colocalization of the fluorescence signals of TRF1 or TRF2 (green) and 53BP1 (red).

(C) The number of TIF spots per cell as a function of the volume of telomeres under various shelterin perturbation conditions. The number of TIF spots per cell correlates strongly (dotted line, Pearson's r = 0.82) with telomere volume.

See also Figures S4 and S5.

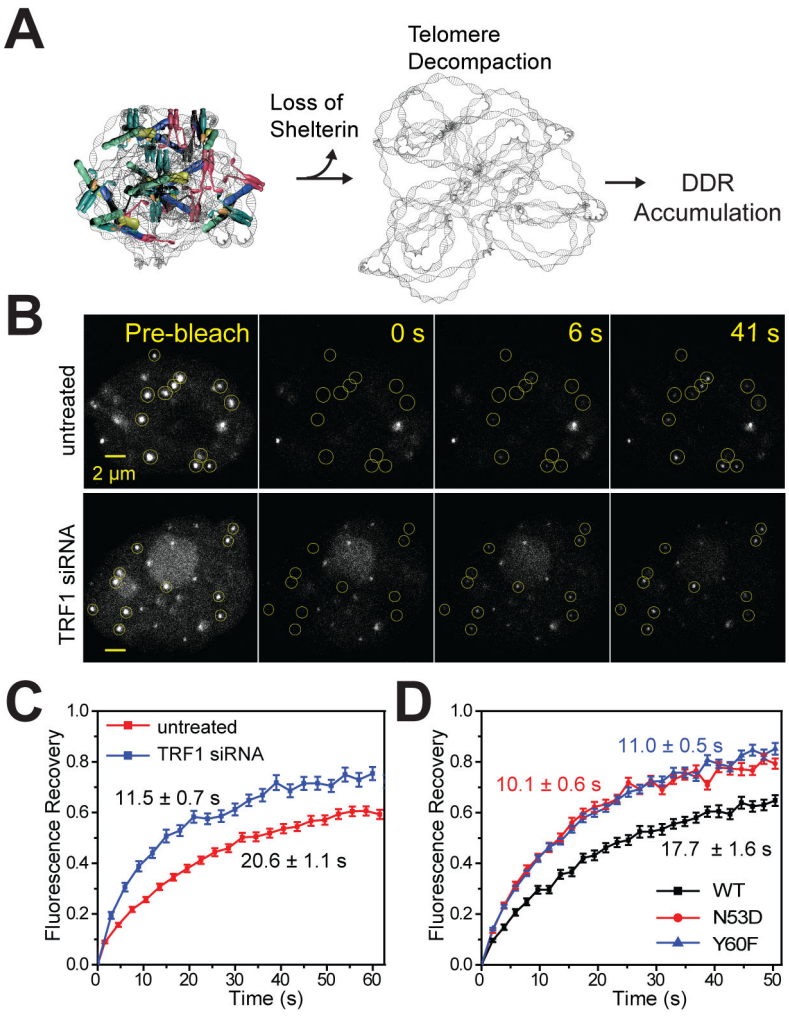

Figure 5. Shelterin-mediated telomere compaction reduces the accessibility of telomere associated proteins

(A) A model for higher-order remodeling of telomeres by shelterin. Shelterin remodels dsTEL tracts into a globular nucleoprotein mesh, which reduces the accessibility of the DDR signals and other telomere-associated proteins to telomeric sites. The removal of shelterin leads to more than a ten-fold decompaction of telomeric chromatin and exposes the protected sites to the DDR signals.

(B) Images of selected time points from FRAP experiments in live HeLa cells expressing GFP POT1 in the absence and presence of TRF1 siRNA treatment. Circular regions covering a single telomere (red circles) were photobleached with a focused laser beam. Images were acquired before bleaching and at 3-s intervals after bleaching, starting at 0 s.

(C) The recovery of GFP-POT1 fluorescence at individual telomeres is faster in TRF1 depleted cells than untreated cells. Values represent mean ± SEM from 15 cells.

(D) Quantitative analysis of the recovery of TRF2 fluorescence at individual telomeres showed that TRFH dimerization mutants recover faster than WT TRF2. Values represent mean ± SEM from 15 cells.

See also Figure S6, Movies S3 and S4.

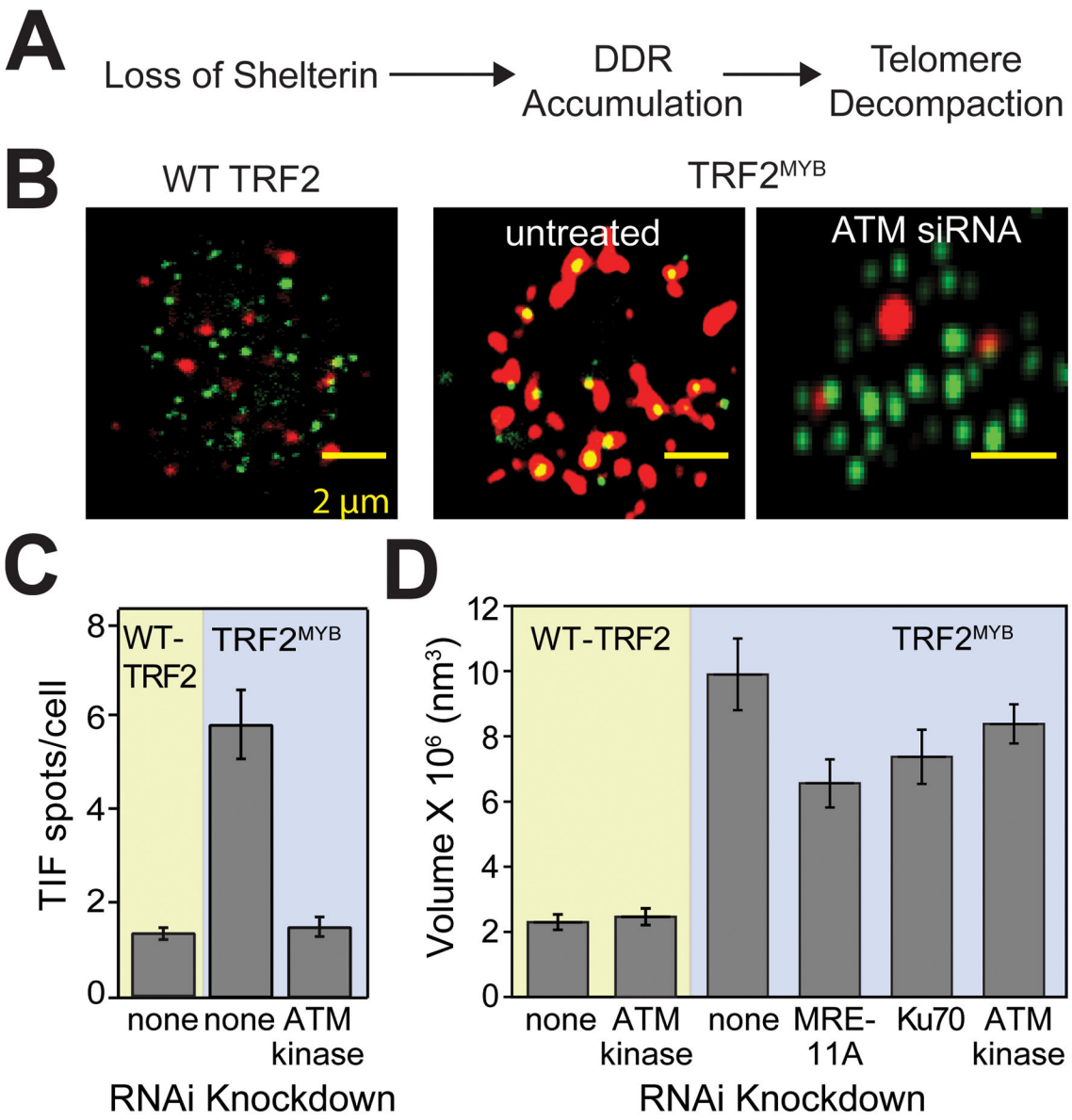

Figure 6. Telomere decompaction upon TRF2 removal is uncoupled from the ATM-pathway

(A) If the accumulation of DDR signals precedes telomere decompaction upon shelterin depletion, inactivation of the DDR pathway would prevent telomere decompaction in shelterin-depleted cells.

(B) The overlay images of telomeres detected by mEos2-TRF2 (green) and the DNA repair sites probed by immunolabeling of 53BP1 with Alexa-647 (red). TIF spots (yellow) were determined by colocalization of the fluorescence signals of TRF1 or TRF2 (green) and 53BP1 (red). $TRF2^{MYB}$ expression leads to a large increase in TIF spots in ATM active cells, but TIF spots are significantly reduced in ATM knockdown cells.

(C) Comparison of the number of TIF spots per cell in WT TRF2 (yellow shade) and $TRF2^{MYB}$ expressing (blue shade) cells. Error bars show SEM. $N_{telomeres}$ is >50 for each case.

(D) Comparison of the telomere volume in WT TRF2 (yellow shade) and $TRF2^{MYB}$ expressing (blue shade) cells. $TRF2^{MYB}$ expression leads to telomere decompaction even in cells depleted of DDR proteins. Error bars show SEM. $N_{telomeres}$ is >150 for each case. See also Figure S6

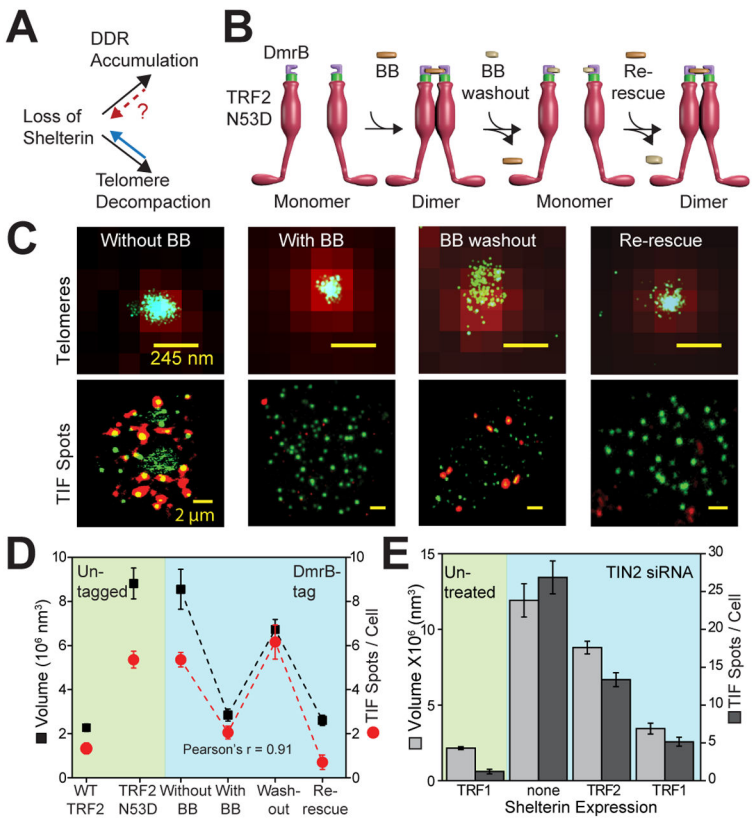

Figure 7. Recompaction of telomeric chromatin reduces TIFs

(A) If DDR accumulation and DNA decompaction occur simultaneously upon the removal of shelterin from telomeres, recompaction of telomeric chromatin using an orthogonal method (blue arrow) would not reduce DDR accumulation (red arrow).

(B) A DmrB tag is fused to the N-terminus of TRF2-N53D. Monomer to dimer transition of TRF2 is controlled by the BB dimerizer and BB washout ligand.

(C) (Top) Representative telomeric structures and (Bottom) TIF spots (yellow; green: TRF2 and red: 53BP1) as monomer to dimer transition of TRF2 is reversibly controlled in HeLa cells.

(D) Telomeric chromatin in DmrB-tagged TRF2-N53D expressing cells is reversibly compacted by dimerization and decompacted by monomerization of TRF2-N53D (blue shaded region). The number of TIF spots per cells correlates strongly (dotted line, Pearson's r = 0.91) with changes in telomere volume in these cells (mean ± SEM). Values for cells expressing WT TRF2 and TRF2-N53D without the DmrB tag are shown for comparison (green shaded region).

(E) Overexpression of TRF1 and TRF2 in TIN2-depleted cells leads to telomere compaction and reduction in the number of TIFs per cell.

See also Figure S7